tation are not yet complete, they clearly show spectrally shifted peaks away from the ruby-laser wavelength. The fact that the scattered radiation is shifted, in addition to the large enhanced signal levels detected, precludes Rayleigh scattering from excited hydrogen atoms as being responsible. Observed signals are at least two orders of magnitude greater than near-resonant Rayleigh scattering from hydrogen could ever provide for our experimental conditions.

Significantly, the scattering was sufficiently enhanced that it was necessary to use 10^3 attenuation in detection to obtain counts within the dynamic range of the analyzer (800 counts). As further evidence of the highly nonthermal nature, a search for the electron feature (several hundred angstroms in width) made by removing the 10^3 attenuation yielded no scattered signal. Since for thermal scattering the peak ion to electron ratio is ~ 10, the detection sensitivity sets a lower bound of ~ 10^4 enhancement over thermal.

In fact, a direct calibration using Rayleigh scattering showed typical enhancements of 10^4–10^5 with occasional shots up to 10^6. Now for the probed $k = 2\pi/\lambda = 9\times10^4$ cm^{-1}, thermal fluctuations would imply density fluctuations $(\delta n/n)_{\rm th} \sim (n\lambda^3)^{-1/2} \sim 10^{-3}$. Thus since the Thomson-scattered signal $\sim |\delta n_k|^2$, an enhancement of 10^4 implies $\delta n_k/n \sim 0.1$ with correspondingly higher values for greater enhanced scattering. Clearly, very large levels of low-frequency ion (and electron) fluctuations have been induced by CO_2-laser heating of the gas-target plasma.

The presence of such fluctuations levels for $k\lambda_D \sim 0.5$ and $\vec{k} \perp \vec{k}_0$ of the CO_2 laser, as well as the experimentally observed $\delta n/n \gtrsim 0.1$ for $k\lambda_D \sim 0.065$ with $\vec{k} = 2\vec{k}_0$, clearly shows significant ion turbulence over a broad geometry and spectral range. Potentially efficient absorption of laser radiation can result from these fluctuations.

Since we have directly measured the fluctuation level for $k\lambda_D \sim 0.5$, it is interesting to calculate the anomalous heating rate ν^* for our plasma assuming $\delta n_k/n \sim 0.1$ to be true for a broad spectrum of k as indicated from our experimental results. Taking $\langle \cos^2\theta_i \rangle \simeq \frac{1}{2}$ and $\langle {\rm Im}\epsilon/|\epsilon|^2 \rangle \simeq 1$ where brackets denote averages over k, we find $\nu^* \sim \nu_{ei}/3$. Evidently fluctuation levels of 20% would make $\nu^* \gtrsim \nu_{ei}$. Thus for short periods during the relatively long-pulse CO_2-laser heating of the underdense plasma, anomalous absorption may very well be contributing to heating.

We wish to thank M. Cervenan, B. Hadley, and P. Haswell for assistance in this experiment.

[1]J. F. Drake, P. K. Kaw, Y. C. Lee, G. Schmidt, C. S. Liu, and M. N. Rosenbluth, Phys. Fluids 17, 778 (1974); D. W. Forslund, J. M. Kindel, and E. L. Lindman, Phys. Fluids 18, 1002 (1975), and references contained therein.

[2]P. K. Kaw and J. M. Dawson, Phys. Fluids 12, 2586 (1969).

[3]R. J. Faehl and W. L. Kruer, Phys. Fluids 20, 55 (1977).

[4]A. A. Offenberger, A. Ng, and M. R. Cervenan, to be published.

[5]A. A. Offenberger, N. H. Burnett, A. R. Strilchuk, and D. F. Way-Nee, Rev. Sci. Instrum. 45, 1400 (1974).

Fast-Ion Emission and Resonance Absorption in Laser-Generated Plasma

P. Wägli and T. P. Donaldson
Institute of Applied Physics, University of Berne, CH-3021-Berne, Switzerland
(Received 18 October 1977)

Plasma was generated by focusing a 35-psec, 1.06-μm laser onto Perspex. Ion expansion characteristics were measured relative to laser polarization and incidence angle. Thermal and "fast" ions were always seen. For optimum resonance absorption conditions the thermal ion energy increased, and a second faster-ion group appeared. Comparison with a computer code showed that the faster ions originated from electron accerleration by an intense electrostatic field.

The investigation of "fast ions" emitted from a laser-generated plasma is an active research topic[1-7] of particular importance for laser fusion.[8] The energy carried by these ions (greater than the thermal expansion energy of the plasma) is generally considered to be the result of ion acceleration by fast electrons. Examples of possible fast-electron sources are resonantly driv-

© 1978 The American Physical Society

en electric fields,[9-13] flux limitation,[14] ponderomotive force in the coronal plasma,[15] and parametric instabilities.[16] Resonantly excited localized electric fields have been demonstrated to accelerate ions in microwave experiments[17]; similar effects are predicted theoretically and by computer simulations[11,12] to occur under favorable plasma conditions.

In this Letter we report the observation of fast-ion acceleration due to resonantly driven electrostatic fields. In contrast to the results of other workers[7] additional fast ions are seen and these are unconnected with resonance effects. Good agreement is obtained between the experimental results and a computer code which models resonance absorption, with electron density profile steepening by electrostatic field pressure.

The experimental configuration is shown in Fig. 1. A 1.06-μm, 35-ps laser pulse was focused by an $f/3.75$ aspheric lens onto the surface of a massive Perspex $(C_5O_2H_8)_n$ slab target, located in vacuum. The focal depth was ± 225 μm and the focal-spot diameter was 80 μm. Discrimination against any noise preceding the main laser pulse was better than 10^{-6}. Experiments were made with low laser intensities, $I_0 \sim 2\times 10^{13}$ W cm^{-2}, to ensure that parametric instability thresholds were not exceeded, at least for the vacuum field values, thus avoiding unnecessary interference with a clear interpretation of the experimental results. The target surface finish was better than $\lambda/4$, and the target was set at an angle, θ, between its normal and the laser beam axis.

By passing the incident laser beam through a half-wave plate its E-vector polarization was continuously variable through an angle, φ, relative to the plane of incidence. Ion emission was detected by Faraday cups. For known ion mass, it was possible to derive ion energy from time of flight. The Faraday cup which viewed plasma along the target normal (0°) was combined with an electrostatic analyzer for energy discrimination.

Ion currents were monitored by oscilloscopes

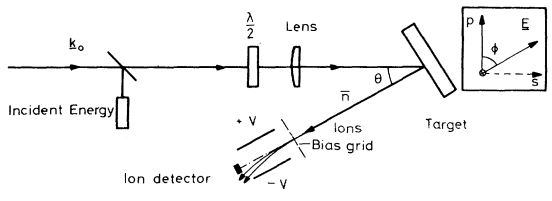

FIG. 1. Experimental configuration.

and measurements were made, using the 0° detector, for a range of laser incidence angles, θ, and for a range of polarization angles, φ, with the target set at $\theta = 20°$, close to the optimum resonance absorption angle of $15° \pm 5°$.[18] For each θ and φ, up to ten current traces were recorded, with the laser intensity, I_0, varying statistically between 1.5×10^{13} and 2.5×10^{13} W cm^{-2}. To illustrate the different ion peaks, a trace, taken on the 0° detector, for $\theta = 20°$, $\varphi = 0°$ (p polarization), without the electrostatic analyzer, is shown in Fig. 2(a). The broad low-energy peak is due to the arrival of thermal plasma. In addition to the thermal peak, two high-energy (fast peaks) can be seen: "fast" and "ultrafast." These show completely different behavior. For example, for a precisely focused target, $\vec{E}$ and $\vec{k}$ vectors are well defined, and the ultrafast ions, shown to be due to resonance effects, are distinctly seen. In contrast, the fast ions, independent of resonance, are not visible. Their disappearance is unlikely to be due to masking by the ultrafast component because they also disappear for s polarization. As the target is moved out of focus, the ultrafast-ion flux diminishes while the fast-ion flux is enhanced.

For the measurements of the ultrafast energy

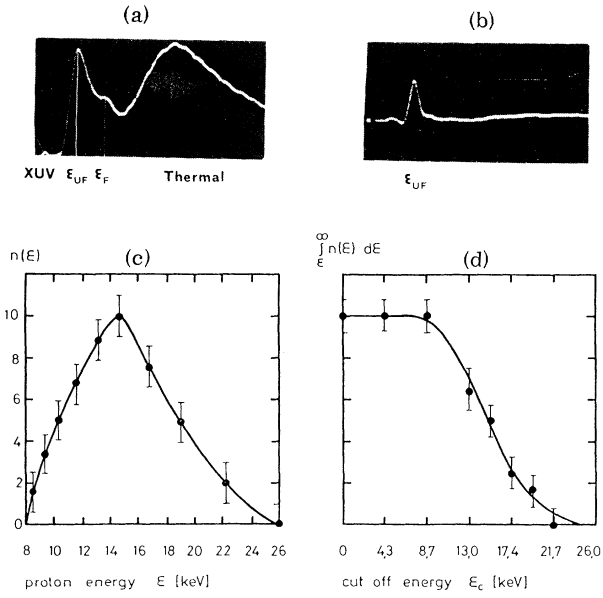

FIG. 2. Ion emission traces and distribution function. (a) Ion trace showing extreme-ultraviolet, nonthermal and thermal ion peaks, (b) ultrafast-ion peak, (c) proton distribution function, (d) the points are the integrated proton distribution function obtained from the electrostatic analyzer measurement. The solid line is the integral of the distribution function in (c).

distribution function, the thermal ions were suppressed by a biased grid (150 V), placed over the electrostatic analyzer entrance. Figure 2(b) shows an example of the ultrafast-ion peak isolated in this way, obtainte with the target precisely in focus so that the fast ions are not visible. Time-of-flight measurements on such a trace yielded the energy distribution function for the ultrafast ions, in arbitrary units [Fig. 2(c)]. The analyzer deflection voltage, V, determines a cutoff energy, ϵ_c, which is defined as the maximum energy of the ions deflected by more than one detector aperture, a. It is related to the voltage by $\epsilon_c = (zx^2/4a)V/d$, where z is ion charge, x is deflection length and d is deflection-plate separation. The integral of the distribution function from ϵ_c to ∞, was measured by varying V, Fig. 2(d). Comparison with the measured distribution yielded the distribution function calibration in absolute energy units. The large peak in Fig. 2(b) consisted of protons and the barely visible peak to the right consisted of C^{6+} and/or O^{8+}. The ultrafast ions were unambiguously shown to be predominantly protons, and so the ultrafast-ion energy, ϵ_{uf}, was taken to be the energy corresponding to the proton distribution peak.

Using an array of five Faraday cups, the thermal ion emission flux for both s and p polarizations was found to be confined to the target normal direction, within an angle of $\pm 15°$. The emission cone for the fast and ultrafast ions was narrower ($\pm 5°$). Thus *meaningful* measurements of the fast- and ultrafast-ion parameters were only obtained by viewing emission along the target normal. All subsequent measurements were therefore made using the 0° detector.

Figure 3(a) shows, as a function of the polarization angle, φ, a plot of the total thermal energy, $\int_0^\infty n(\epsilon_T)\epsilon_T\, d\epsilon_T$, normalized to 1, for $I_0 = 2\times 10^{13}$ W cm^{-2} and $\theta = 20°$. This was derived from the thermal ion peak, assuming an average ion charge of 3.5, and is a measure of the original thermal electron energy in the plasma, transferred to the ions by adiabatic expansion. The enhancement towards p polarization follows a $\cos^2\varphi$ law, consistent with resonance absorption of the laser radiation, since $I_0 \sim E_0^2\cos^2\varphi$, where E_0 is the vacuum laser electric field. The same functional dependence was found for the directly measured enhancement of the "cold"-electron temperature, from 150 to 235 eV, under the same plasma conditions (Ref. 18). It can be seen from the work of Donaldson, Hutcheon, and Key[19] that the average ion charge changes by no more than a factor of 1.15 over this temperature range. Energy gained by resonance is damped in the plasma and enhances the cold-electron temperature. The observed enhancement [Fig. 3(a)] is consistent with a calculated inverse bremsstrahlung absorption of 25% and a maximum resonance absorption of half the remaining energy which reaches the critical surface. This result was also obtained from the direct measurement of the cold-electron–temperature enhancement in Ref. 18.

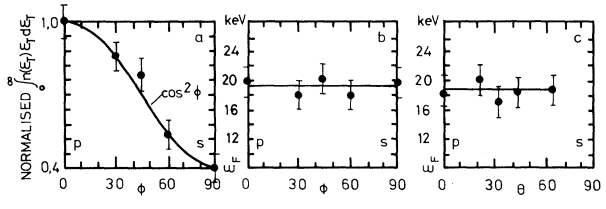

FIG. 3. Thermal- and fast-ion emission behavior, (a) total thermal energy, normalized to 1, obtained from the thermal peak, (b) fast-ion energy φ dependence, (c) fast-ion energy θ dependence.

Using the electrostatic analyzer, the energy per charge of the fast ions was found to be 8–10 keV/z. By comparison with time of flight they were identified as C^{2+}. In Figs. 3(b) and 3(c), the energy of the fast peak, ϵ_f, is shown. Measurements were made with the target $\simeq 150$ μm out of focus. ϵ_f can be seen to be independent of both the polarization and incidence angles. This implies that the electrons which accelerate these ions do not originate from the resonance region. ϵ_f was found to increase with laser intensity, as $I_0^{1/4}$, so that, although ϵ_f is insensitive to the direction of the E vector, it is sensitive to its absolute magnitude.

Different behavior can be seen for the ultrafast-ion energy, ϵ_{uf}, plotted as a function of φ in Fig. 4(a), for $\theta = 20°$. Figure 4(b) shows the variation

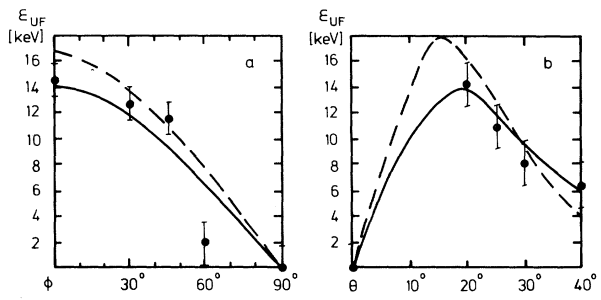

FIG. 4. Ultrafast-ion behavior: (a) dependence of ultrafast-ion energy on polarization angle, φ; (b) dependence of ultrafast-ion energy on incidence angle, θ.

with θ of ϵ_{uf} for p-polarized radiation. It can be seen that ϵ_{uf} increases from zero, at $\theta = 0°$ to a peak value of 14.5 keV, at $\theta = 20°$, and falls to 6.5 keV at $\theta = 40°$. (Cf. the resonance absorption peak at 15° found from direct measurement of T_e, Ref. 18.) Since the ultrafast ions are protons, the source electrons will have the same average energy. The source electrons can only be accelerated to these energies if an electric field much greater than the driver electromagnetic field exists. An intense localized spike of *electrostatic* field can be driven by the electromagnetic field in the critical region, where it is resonant with plasma waves.[11,12] If collisional damping is low in this localized region, the maximum possible electrostatic field is limited by plasma wave convection to $E_{max} = E_d(L/\lambda_{De})^{2/3}$,[11] where λ_{De} is the Debye length in the resonance region.

These results were compared with the predictions of the computer code, ZWERG, which models resonance absorption and resonance field generation. This code, described in more detail elsewhere,[20] solves a self-consistent set of equations for energy and momentum balance. Absorption is by inverse bremsstrahlung and plasma resonance, while energy is lost through thermal and nonthermal ion convection. The resonance field is limited by plasma wave convection, and self-consistent steepening of the electron density gradient is described by the inclusion of *electrostatic* field pressure in the momentum balance. The code predictions for ϵ_{uf} as a function of θ and φ are represented in Fig. 4 by continuous curves. They are in good agreement with the measured values, in contrast to the code predictions when steepening is not included (dashed curves).

It can be seen, Fig. 4(b), that the main effect of profile steepening by the electrostatic field is to reduce the maximum ultrafast-ion energy. This is due mainly to the shortening of the acceleration length. At high incidence angles the steepening shows a tendency to maintain the resonance and keep ϵ_{uf} finite.

At $I_0 = 2 \times 10^{13}$ W cm^{-2}, p polarization and $\theta = 20°$, the code predicts a value of $E_{max} = 10^9$ V cm^{-1}, a field extent of 10^{-5} cm and $\epsilon_{uf} = 14.5$ keV. Note that intense electric field spikes have also been inferred in CO_2-laser experiments, where resonance absorption was thought to play a significant role in the absorption of the laser radiation.[21-23] The total energy carried by the ultrafast ions, at a laser irradiance of 2×10^{13} W cm^{-2}, was measured to be 15% of the energy carried by the thermal ions. The trend was towards a higher fraction of energy transport by fast-ion convection at higher laser intensities.

In conclusion, it has been demonstrated that the thermal ion peak is enhanced on resonance, a result consistent with resonance absorption. Two fast-ion peaks occur for p polarization, while only one occurs for s polarization. Their behavior is sufficiently different to allow them to be distinguishable. The ultrafast-ion peak appears only when the conditions for resonance absorption are favorable, and its acceleration source is a localized spike of resonantly generated electrostatic field, as predicted by computer simulations. Protons were seen to be preferentially accelerated.[24] Evidence was obtained for steepening of the electron density profile by the electrostatic field pressure.

The authors would like to thank Professor H. P. Weber for the provision of research facilities and his interest in the work, the Swiss National Science Foundation for their funding of the work, J. E. Balmer and P. Lädrach for assistance with the experiment, and M. Colomb and M. Fuhrer for assistance with the laser system.

[1]P. Koch and J. Albritton, Phys. Rev. Lett. 32, 1420 (1974).
[2]V. P. Silin, Pis'ma Zh. Eksp. Teor. Fiz. 21, 333 (1975) [JETP Lett. 21, 152 (1975)].
[3]G. H. McCall, F. Young, A. W. Ehler, J. F. Kephart, and R. P. Godwin, Phys. Rev. Lett. 30, 1116 (1973).
[4]A. W. Ehler, J. Appl. Phys. 46, 2464 (1975).
[5]J. Martineau, P. Paranthoën, M. Rabeau, and C. Patou, Opt. Commun. 15, 404 (1975).
[6]R. A. Haas, W. C. Mead, W. L. Kruer, D. W. Phillion, H. N. Kornblum, J. D. Lindl, D. Mac Quigg, V. C. Rupert, and K. G. Tirsell, Phys. Fluids 20, 322 (1977).
[7]J. S. Pearlman, J. J. Thomson, and C. E. Max, Phys. Rev. Lett. 38, 1397 (1977).
[8]J. Nuckolls, L. Wood, A. Thiessen, and G. Zimmerman, Nature (London) 239, 139 (1972).
[9]J. P. Freidberg, R. W. Mitchell, R. L. Morse, and L. I. Rudsinski, Phys. Rev. Lett. 28, 795 (1972).
[10]D. W. Forslund, J. M. Kindel, K. Lee, E. L. Lindman, and R. L. Morse, Phys. Rev. A 11, 679 (1975).
[11]K. G. Estabrook, E. J. Valeo, and W. L. Kruer, Phys. Fluids 18, 1151 (1975).
[12]J. S. DeGroot and J. E. Tull, Phys. Fluids 18, 672 (1975).
[13]P. Kolodner and E. Yablonovitch, Phys. Rev. Lett. 37, 1754 (1976).
[14]R. C. Malone, R. L. McCrory, and R. L. Morse,

Phys. Rev. Lett. 34, 721 (1975).
[15]H. Hora, in *Laser Interaction and Related Plasma Phenomena*, edited by H. J. Schwarz and H. Hora (Plenum, New York, 1971), Vol. 1, p. 383.
[16]J. J. Thomson, R. J. Faehl, W. L. Kruer, and S. Bodner, Phys. Fluids 17, 973 (1974).
[17]A. Y. Wong and R. L. Stenzel, Phys. Rev. Lett. 34, 727 (1975).
[18]J. E. Balmer and T. P. Donaldson, Phys. Rev. Lett. 39, 1084 (1977).
[19]T. P. Donaldson, R. J. Hutcheon, and M. H. Key, J. Phys. B 6, 1525 (1973).
[20]P. Wägli, T. P. Donaldson, and P. Lädrach, to be published.
[21]T. P. Donaldson and I. J. Spalding, Phys. Rev. Lett. 36, 467 (1976).
[22]T. P. Donaldson, M. Hubbard, and I. J. Spalding, Phys. Rev. Lett. 37, 1348 (1976).
[23]T. P. Donaldson, I. J. Spalding, and R. A. Woolley, Opt. Commun. 22, 207 (1977).
[24]R. Decoste and B. H. Ripin, Phys. Rev. Lett. 40, 34 (1978).

Anomalous Absorption in Amorphous Solids at Low Temperature

M. A. Bösch[a]
Laboratory of Atomic and Solid State Physics, Cornell University, Ithaca, New York 14853
(Received 9 December 1977)

Highly absorbing silica-based glasses exhibit a distinct minimum in the temperature dependence of the very-far-infrared absorption coefficient near 10 K. The associated anomalous absorption at lower temperature can be understood by the two-level tunneling model. Different amorphous materials manifest a considerable diversity in the anomalous behavior.

Amorphous solids exhibit thermal and elastic properties at *low* temperatures very different from those of pure crystalline solids. The specific heat is anomalously high and dominated by a term with a linear temperature dependence,[1] indicating the existence of low-energy excitations. Such universal features—like the almost quadratic temperature dependence of the thermal conductivity—independent of structural details have led to the assumption of an universal origin inherent in the disordered state. A statistical distribution of localized two-level tunneling systems[2] (TLS) can describe phenomenologically these anomalous properties at low temperatures. The TLS are viewed as structural or electronic[3] "centers" with two equilibrium configurations, where transitions between the two sites are possible by quantum mechanical tunneling at low temperature and by thermally activated processes at higher temperature. Saturation of the ultrasonic absorption and coherent resonance phenomena[4] have been observed, supporting the tunneling model.

In contrast to the above features the interaction of the electromagnetic field with the TLS is expected to be quite sensitive to the chemical composition of the amorphous material. An anomalous dielectric dispersion[5] as well as a temperature-dependent far-infrared absorption difference[6] has been reported but these measurements dealt with systems which have small intrinsic dipole moments so that intrinsic effects associated with the TLS were masked by the OH^- absorption processes.

For the first time I directly observe an anomalous absorption with an associated minimum in the temperature dependence of the absorption coefficient. Furthermore, highly absorbing glasses have allowed me to observe an anomalous absorption also below 1 K, in contrast to previous results.[6] This Letter is intended (1) to present the experimental data showing the anomalous behavior and the applicability of the two-level tunneling model; (2) to show that several absorption processes contribute to the overall dielectric absorption; (3) to point out the considerable diversity in the anomalous properties of amorphous solids.

A spectrometer system, including a lamellar interferometer, liquid-He^3–cooled detector and a separate He^3-cooled sample section permitted to measure the transmissivity for temperature between 0.4 and 300 K in the frequency interval from 2 to 20 cm^{-1} (VFIR). Three main classes of amorphous substances have been investigated: oxide glasses, polymers, and amorphous semiconductors.

The VFIR frequency dependence of the absorption coefficient α of a soda-lime-silica glass (SLS) is shown in Fig. 1 for various tempera-

© 1978 The American Physical Society

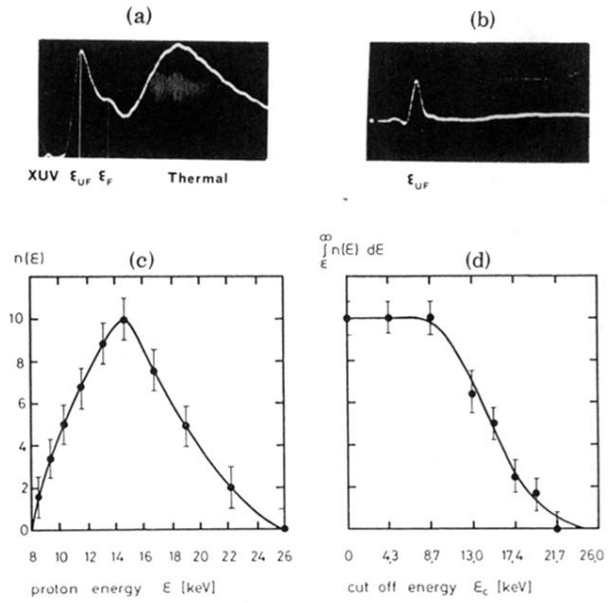

FIG. 2. Ion emission traces and distribution function. (a) Ion trace showing extreme-ultraviolet, nonthermal and thermal ion peaks, (b) ultrafast-ion peak, (c) proton distribution function, (d) the points are the integrated proton distribution function obtained from the electrostatic analyzer measurement. The solid line is the integral of the distribution function in (c).